Selective Inactivation of c-Jun NH_2-Terminal Kinase in Adipose Tissue Protects Against Diet-Induced Obesity and Improves Insulin Sensitivity in Both Liver and Skeletal Muscle in Mice

Xinmei Zhang,[1,2] Aimin Xu,[1,2,3] Sookja K. Chung,[2,4] Justin H.B. Cresser,[5] Gary Sweeney,[5] Rachel L.C. Wong,[1] Anning Lin,[6] and Karen S.L. Lam[1,2]

OBJECTIVE—Obesity is associated with increased activation of the c-Jun NH_2-terminal kinase (JNK) in several metabolic organs, including adipose tissue, liver, and skeletal muscle. In this study, we aimed to define the role of JNK activation in adipose tissue in the development of obesity-related insulin resistance.

RESEARCH DESIGN AND METHODS—Transgenic mice with adipose tissue–specific overexpression of dominant-negative JNK (*ap2-dn-JNK*) under the transcriptional control of the aP2 gene promoter were generated and subjected to metabolic characterization together with the wild-type littermates.

RESULTS—On a high-fat diet (HFD), the *ap2-dn-JNK* mice displayed a marked suppression of both JNK1 and JNK2 activation in their adipose tissue, accompanied by a marked reduction in weight gain, fat mass, and size of the adipocytes. The transgenic mice were resistant to the deleterious impact of an HFD on systemic insulin sensitivity, glucose tolerance, and hepatic steatosis. Reduced hepatic gluconeogenesis was evident in in vivo and ex vivo studies and showed greater insulin-induced glucose uptake in skeletal muscles. These changes were accompanied by reduced macrophage infiltration in adipose tissue, decreased production of proinflammatory adipokines, and increased expression of adiponectin. Indirect calorimetry analysis showed that the transgenic mice had significant increases in oxygen consumption and reductions in respiration exchange rates compared with their wild-type littermates.

CONCLUSIONS—Selective suppression of JNK activation in adipose tissue alone is sufficient to counteract HFD-induced obesity and its associated metabolic dysregulations, in part through an increase in energy expenditure and a decrease in systemic inflammation. ***Diabetes*** **60:486–495, 2011**

From the [1]Department of Medicine, Li Ka Shing Faculty of Medicine, University of Hong Kong, Hong Kong; the [2]Research Center of Heart, Brain, Hormone, and Healthy Ageing, Li Ka Shing Faculty of Medicine, University of Hong Kong, Hong Kong; the [3]Department of Pharmacology and Pharmacy, Li Ka Shing Faculty of Medicine, University of Hong Kong, Hong Kong; the [4]Department of Anatomy, Li Ka Shing Faculty of Medicine, University of Hong Kong, Hong Kong; the [5]Department of Biology, York University, Toronto, Canada; and the [6]Ben May Department for Cancer Research, University of Chicago, Chicago, Illinois.

Corresponding author: Karen Lam, ksllam@hku.hk, or Aimin Xu, amxu@hku.hk.

Received 6 May 2010 and accepted 14 November 2010.

DOI: 10.2337/db10-0650

This article contains Supplementary Data online at http://diabetes.diabetesjournals.org/lookup/suppl/doi:10.2337/db10-0650/-/DC1.

Obesity is a major risk factor of type 2 diabetes. Although the detailed molecular events linking obesity to type 2 diabetes are not well understood, mounting evidence suggests that chronic inflammation in the adipose tissue plays a major role (1,2). Systemic inflammation, characterized by elevated circulating concentrations of proinflammatory markers such as C-reactive protein, is frequently observed in obesity and predicts the development of type 2 diabetes (3). Adipose tissue is now recognized as the predominant contributor of systemic inflammation observed in obese states. Obesity is associated with macrophage infiltration in adipose tissue (4) and dysregulated production of adipokines (2,5), with increased production of proinflammatory adipokines/cytokines, which induce insulin resistance, such as tumor necrosis factor (TNF)-α, interleukin (IL)-6, monocyte chemotactic protein (MCP)-1, and adipocyte fatty acid–binding protein (A-FABP), and decreased production of adiponectin, an anti-inflammatory and insulin-sensitizing adipokine.

Recent studies (2,6) in rodents suggest that c-Jun NH_2-terminal kinase (JNK) is a key player in adipose tissue inflammation and provides a link between nutrient excess, inflammation, and impaired insulin signaling. The JNK group of serine/threonine kinases, JNK1, -2, and -3, belongs to the mitogen-activated protein kinase family (7); JNK1 and JNK2 are widely distributed, whereas JNK3 is restricted to the brain, heart, testis, and pancreatic islets. Through the phosphorylation of various transcription factors, including c-Jun and JunB, JNKs are involved in the regulation of development, immune response, cell survival, and apoptosis (7). Recently, it has been observed that in *ob/ob* rodents JNK activity is increased in liver, muscle, and, markedly, in adipose tissue (8). This is not unexpected because various stimuli that activate JNK, including fatty acids, cytokines (notably TNF-α), and endoplasmic stress (9), are increased in obesity. Activated JNK induces serine phosphorylation of insulin receptor substrate-1 at Ser307, which suppresses tyrosine phosphorylation, leading to impaired insulin action. Genetic deletion of *JNK1* is associated with reduced adiposity and protection against insulin resistance and type 2 diabetes in both diet-induced and genetic obesity, as well as increased adiponectin levels and reduced expression of proinflammatory cytokines (8,10). Adenovirus-mediated delivery of dominant-negative JNK (dn-JNK) or wild-type JNK in *ob/ob* mice has confirmed the role of JNK activation

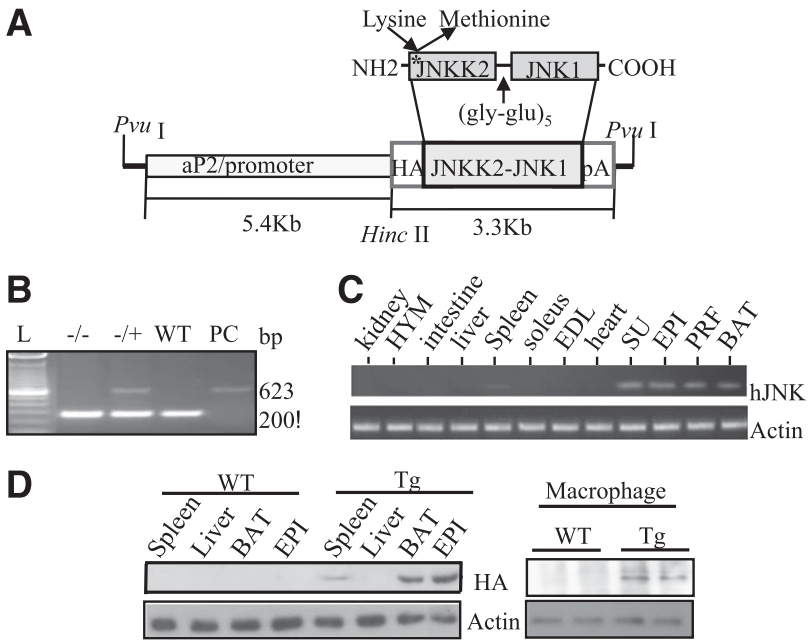

FIG. 1. Generation and characterization of *aP2-dn-JNK* transgenic (Tg) mice. *A*: Schematic representation of the *aP2-dn-JNK* transgenic construct. The *dn-JNK* cDNA, in which lysine 149 in the ATP domain of the JNKK2 moiety was replaced by Met to create the HA-*JNKK2(K149M)JNK1*, was subcloned downstream of the 5.4-kb aP2 promoter/enhancer and upstream of the hGH polyadenylation signals. *B*: Detection of the *dn-JNK* transgene by PCR analysis in mice. Specific fragments of 653 bp spanning from the *aP2* promoter to the *JNKK2* gene was amplified. $^{-/-}$, transgene negative; $^{-/+}$, transgene positive; L, 1-kb DNA ladder; PC, plasmid DNA positive control; WT, wild-type littermates. *C*: Expression of the *dn-JNK* transgene by RT-PCR. The presence of the *dn-JNK* mRNA was analyzed in various tissues of *aP2-dn-JNK* transgenic mice (10 weeks old) by RT-PCR using specific primers for the *dn-JNK* transgene (n = 5). EPI, epididymal adipose fat; PRF, perirenal fat; SU, subcutaneous adipose fat. *D*: Confirmation of the *dn-JNK* protein expression by immunoblotting (n = 4). Protein extracts from various tissues were subjected to Western blotting with anti-HA antibody.

in the liver in enhancing systemic insulin resistance through increasing hepatic glucose output (11). More recently, targeted deletion of *JNK1* in the muscle (12) and reciprocal adoptive transfer experiments (13) show that *JNK1* in muscles and macrophages also contribute to insulin resistance, but not adiposity, in mice with high-fat diet (HFD)-induced obesity. On the other hand, adipocyte-specific deletion of *JNK1* improves insulin sensitivity in the liver and adipose tissue but, again, has no impact on adiposity (14).

The improvement in insulin resistance in *ob/ob* mice after treatment with selective inhibitors of JNKs (6,15) suggests that the suppression of JNK activation is an attractive therapeutic approach in the management of obesity-related type 2 diabetes. In this study, using an alternative strategy of JNK inactivation, we have demonstrated, for the first time, that selective suppression of both JNK1 and JNK2 activation in adipose tissue alone can protect against both increased adiposity and insulin resistance induced by an HFD.

RESEARCH DESIGN AND METHODS

Antibodies and chemicals. Rabbit polyclonal antibodies against total JNK1/2 and phospho-JNK1/2 and total Akt and phosphor-Akt (Thr308) were from Cell Signaling Technology, and antibodies against hemagglutinin (HA) tag and β-actin were from Sigma. Murine monoclonal antibody against F4/80 was from Serotec. The JNK Activity Assay Kit was purchased from Abcam. Glucose, insulin, and sodium pyruvate were from Sigma. [1-^{14}C]Oleic acid, [^{14}C]mannitol, and 2-deoxy-D-[^{3}H]glucose were purchased from Amersham.

Generation of transgenic mice. A 3.3-kb cDNA fragment encoding HA-tagged JNKK2 (KM)-JNK1 fusion protein, in which lysine 149 in the ATP domain of the JNKK2 moiety was replaced by methionine, was released from the pSRα3HA-JNKK2 (K149M)-*JNK1* construct (16) by digestion with *Bgl* I and *Hind* III and was then subcloned into a transgenic vector under the control of the 5.4-kb aP2 promoter (17). The transgenic vector was digested by *Pvu* I, and an 8.7-kb fragment carrying the *aP2* promoter and the transgene was isolated and microinjected into the pronucleus of fertilized eggs of C57BL/6×CBA mice, as described previously (17). Transgenic founders were identified by PCR analysis using a pair of primers listed in Supplemental Table 1. Four independent transgenic lines were established. The transgenic founders were backcrossed with C57BL/6J for at least six generations. All experimental procedures were approved by the committee on the use of live animals for teaching and research of the University of Hong Kong and were carried out in accordance with the guide for the care and use of laboratory animals.

Animal maintenance and metabolic studies. The transgenic mice and wild-type littermates were maintained on 12-h light and dark cycles under controlled environmental settings (23 ± 1°C), with free access to water. All experiments were conducted on littermate-controlled male mice with a uniform C57BL/6 J background. In this study, all mice, starting at the age of 4 weeks, were maintained on a standard chow (13% of calories from fat, D5053; LabDiet) or an HFD (45% of calories from fat, D12451; Research Diets) for 20 weeks. Glucose tolerance tests, insulin tolerance tests, and pyruvate tolerance tests were conducted as previously described (18). Blood glucose levels were determined in tail blood using the Ascensia Elite XL blood glucose meter (Bayer Health Care). Fasting serum triglycerides and free fatty acid levels were analyzed with Triglyceride Liquicolor (Stanbio Laboratory) and the Free Fatty Acid Half Micro Test (Roche), respectively. Serum insulin, leptin, A-FABP, and adiponectin levels were determined using enzyme-linked immunosorbent assay kits (Mercodia and Biovender).

Isolation and culture of murine peritoneal macrophages. Peritoneal macrophages were prepared from *ap2-dn-JNK* mice and their wild-type littermates that had previously been injected with 2 mL Brewer thioglycollate broth medium (4 g/100 mL) (Difco Laboratories) for 2 days followed by lavage of the peritoneal cavity with 5 mL of PBS. The peritoneal cells were washed twice and seeded at densities of 6×10^5 cells/mL in RPMI-1640 medium (Gibco) containing 10% (vol/vol) FCS. The macrophages were allowed to adhere for 3 ± 4 h in a 5% CO_2-humidified atmosphere prior to assay for the JNK activity.

JNK activity assay. JNK activity in peritoneal macrophages and adipose tissue was examined via immunoprecipitation of JNK kinase and incubation with the substrate glutathione *S*-transferase (GST)-c-Jun immobilized on GST-agarose beads, following the instructions of the JNK activity assay kit from Abcam. After incubation with an antibody specific to JNK1 and JNK2 for

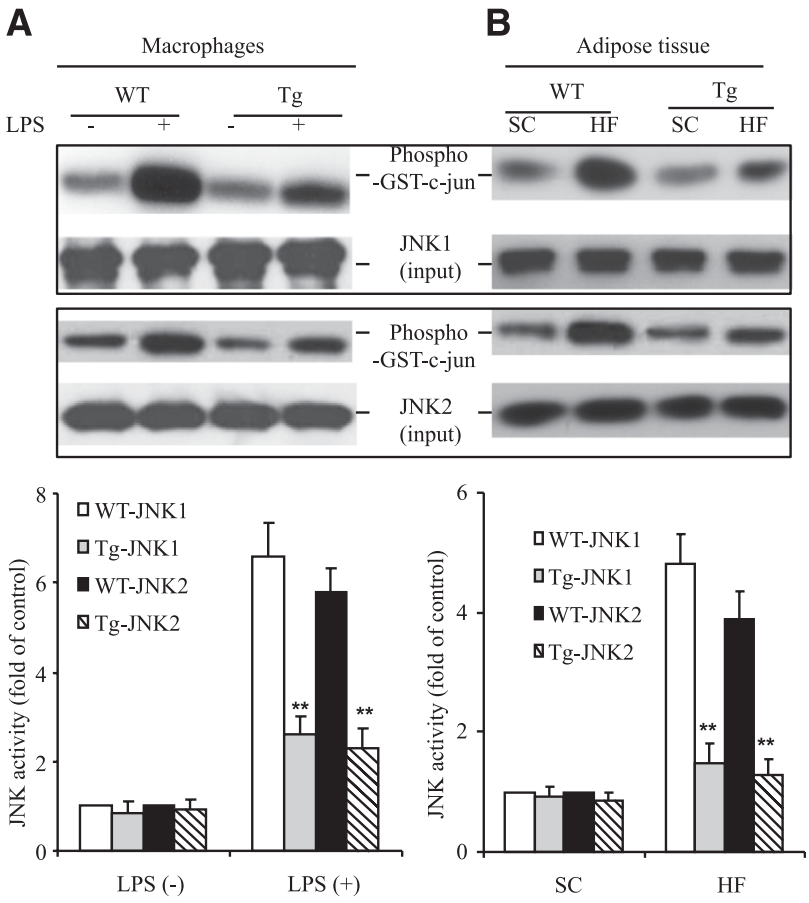

FIG. 2. The activity of both JNK1 and JNK2 was reduced in peritoneal macrophages and adipose tissue of *aP-2dn-JNK* transgenic (Tg) mice. *A*: Cell lysates harvested from peritoneal macrophages stimulated with or without LPS (100 ng/mL, 10 min) were subjected to immunoprecipitation using an antibody specific to JNK1 or JNK2, followed by JNK activity assay using GST–c-Jun as a substrate. *B*: Epididymal fat from *aP2-dn-JNK* or wild-type (WT) littermates on the standard chow (SC) or the HFD for 8 weeks were homogenized and assayed for the activity of JNK1 and JNK2 as in *A*. The bar charts below the blots were the quantitative analysis of JNK1 and JNK2 activity. IB, immunoblots. **$P < 0.01$ vs. wild-type littermates ($n = 5$).

45 min and with protein A-Sepharose for 1 h at room temperature, the beads were washed extensively in a lysis buffer, followed by a kinase assay buffer, and the activity of the bound JNK was detected with the addition of c-Jun protein/ATP for 4 h at 30°C. The reaction products were subjected to SDS-PAGE separation, and the phosphorylated c-Jun protein was detected using the rabbit anti–phospho–c-Jun (Ser73)-specific antibody.

Measurement of [^{3}H]2-deoxyglucose uptake in skeletal muscle and primary adipocytes. Basal and insulin-stimulated glucose uptake was measured as described (19), with a few modifications. The soleus and the extensor digitorum longus muscles were carefully excised from anesthetized mice and incubated for 20 min at 30°C in 2 mL of pregassed (95% O_2, 5% CO_2) Krebs-Henseleit buffer (KHB) containing 0.1% BSA, 8 mmol/L glucose, and 32 mmol/L mannitol. Muscles were then transferred to a glucose-free KHB buffer containing 0.1% BSA, 4 mmol/L pyruvate, and 36 mmol/L mannitol and incubated in the presence or absence of 60 μU/mL insulin for 20 min. Afterward, muscles were incubated for 20 min in a similar KHB buffer containing 2-deoxy-D-[^{3}H]glucose (2.25 μCi/mL) and [^{14}C]mannitol (0.3 μCi/mL) in the presence or absence of insulin. After all incubations, muscle strips were removed, trimmed of tendons, blotted to remove excess fluid, and weighed. The muscle samples were then digested in 1 mL of 1 mol NaOH for 10 min at 95°C. A total of 200 μL of the digested muscle was then subjected to liquid scintillation counting to calculate the intracellular accumulation of 2-deoxy-D-[^{3}H]glucose. Glucose uptake in primary adipocytes isolated from epididymal adipose tissue was described elsewhere (17).

Indirect calorimetry. Mice were individually housed in metabolic chambers maintained at 20–22°C in a 12-h light/12-h dark cycle. Six-week-old mice were fed with an HFD and tap water ad libitum using a computer-controlled open-circuit indirect calorimetry system (Oxymax; Columbus Instruments) with an airflow of 0.6 L/min and sample flow of 0.5 L/min. After the mice had adapted to the environment of the metabolic chamber for 48 h, metabolic parameters (whole-body oxygen consumption rates and respiration exchange rates) were assessed as described (17).

Quantitative real-time PCR. Total RNA from various organs of mice was isolated using the TRIzol reagent (Invitrogen) and treated with RNase-free DNase (Promega, Madison, WI) at 37°C for 30 min to remove genomic DNA and was then subjected to reverse transcription and real-time PCR analysis on an ABI Prism 7000 instrument (Applied Biosystems), as described (17,20). Primers used for real-time PCR are listed in Supplemental Table 1.

Immunohistochemistry and histological analysis. Adipose tissue was fixed in freshly prepared 4% paraformaldehyde in PBS overnight at 4°C and embedded in paraffin for thin sectioning. Immunocytochemistry analysis for macrophage markers and Oil red O staining analysis for lipid accumulation in the liver sections were detailed elsewhere (17,21).

Statistical analysis. The data were expressed as means ± SE. Statistically significant differences between two groups were assessed by one-way ANOVA or the Student t test, as appropriate. A P value <0.05 indicated a significant difference.

RESULTS

Transgenic mice with adipose tissue–specific overexpression of dn-JNK exhibit lipopolysaccharide (LPS) reduced JNK activity in obese adipose tissue and LPS-stimulated peritoneal macrophages. First, we generated transgenic mice overexpressing HA-tagged dn-JNK under the transcriptional control of the A-FABP gene (*aP2*) promoter, which has been routinely used to drive adipose tissue–specific expression of foreign genes in transgenic mice (22). JNKK2 (KM), in which methionine (Met) replaces (Lys) 149 in the ATP-binding domain of c-Jun NH_2-terminal kinase kinase2 (JNKK2) that stimulates JNK activation, has been demonstrated to result in the

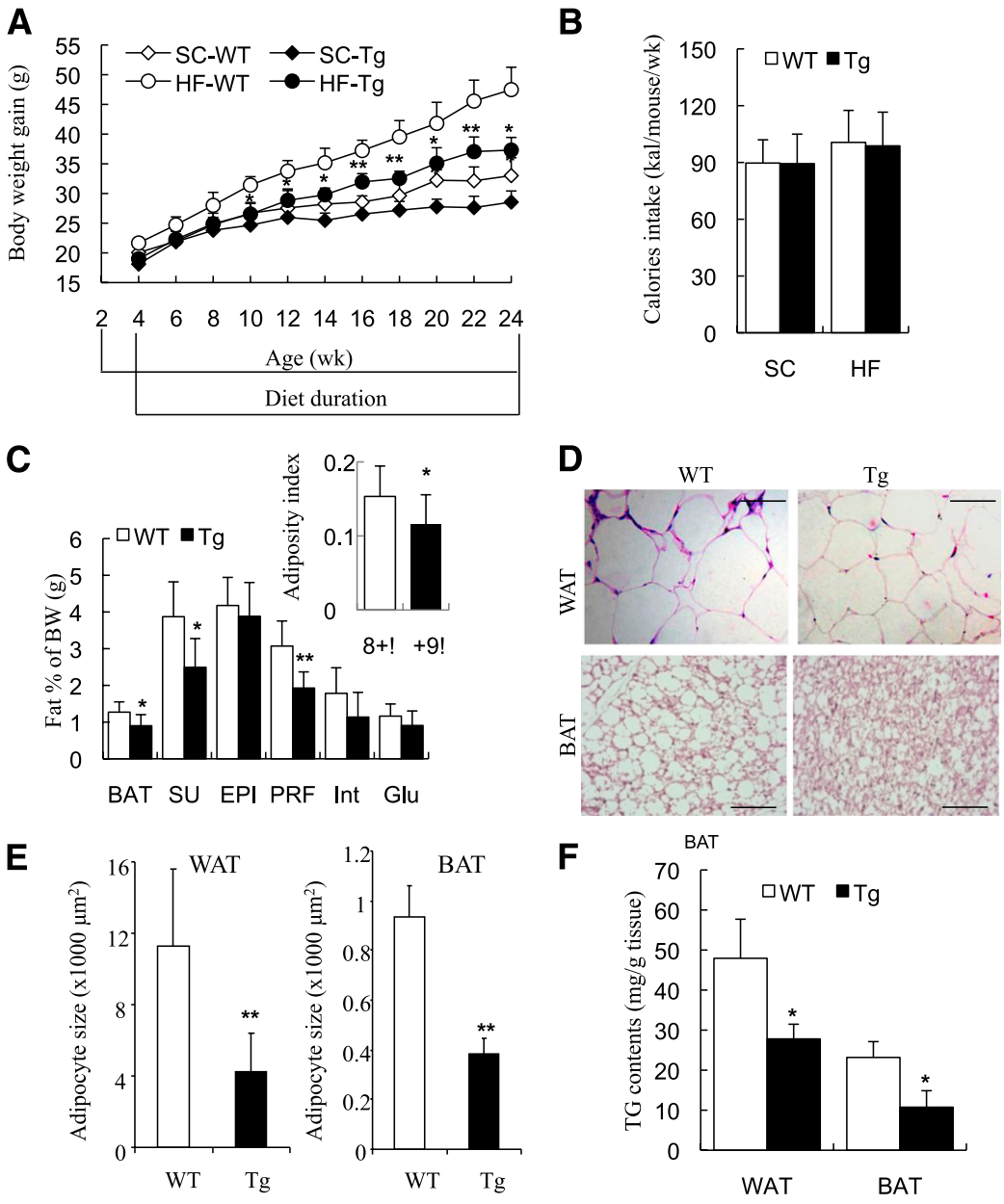

FIG. 3. The *aP2-dn-JNK* mice were less obese than control mice under the HFD, displaying decreased fat mass and triglyceride contents in adipose tissue. *A*: Body weight changes on standard chow (SC) or HFD (HF) over 24 weeks in *aP2-dn-JNK* transgenic (Tg) mice and their wild-type (WT) littermates. *B*: Caloric intake, as calculated by food intake per mouse per week (g/mouse/week) × 3.07 kcal/g on the standard chow and × 4.73 kcal/g on the HFD. *C*: Fat-pad weights in *aP2-dn-JNK* and wild-type littermates, as measured after dissection at the age of 24 weeks and presented as percentage of total body weight. *Insert*: Adiposity index, calculated as the total weight of fat pads divided by total body weight. Fat pads: BAT, subcutaneous (SU), epididymal (EPI), perirenal (PRF), interscapular (Int), WAT, and gluteal fat (Glu). *D*: Representative images of hematoxylin and eosin–stained sections of epididymal WAT and interscapular BAT on the HFD at the age of 24 weeks. Scale bar: 50 μm. *E*: The size of adipocytes quantified using NIH ImageJ software. *F*: Triglyceride contents in epididymal fat pads and brown fat pads. *$P < 0.05$; **$P < 0.01$ vs. wild-type littermates ($n = 6$–8). *A* and *B* were analyzed by ANOVA; *C*, *E*, and *F* were analyzed by the Student *t* test. (A high-quality color representation of this figure is available in the online issue.)

inactivation of JNK (16). Thus, the JNKK2 (KM)-JNK1 fusion protein, dn-JNK, functions as a dominant-negative Jun kinase by competing with endogenous JNK1/2. Our transgenic construct consisted of 5.4 kb of the 5′ flanking fat-specific regulatory region of the *aP2* gene and 21 bp of its first exon and the cDNA of *dn-JNK* (Fig. 1*A*). The transgenic construct was introduced into pronuclei, and four transgenic founders were identified by genotyping (Fig. 1*B*). Both mRNA and protein expression of *dn-JNK* were restricted mainly in white adipose tissue (WAT) and brown adipose tissue (BAT) (Fig. 1*C* and *D*, *left panel*) and in isolated peritoneal macrophages of the transgenic mice (Fig. 1*D*, *right panel*). On the contrary, neither the mRNA nor protein of the transgene was detectable in a panel of other major insulin-responsive tissues, except for a trace amount of *dn-JNK* expression in the spleen.

The transgenic expression of *dn-JNK* had no obvious effect on the activity of either JNK1 or JNK2 in unstimulated peritoneal macrophages (Fig. 2*A*) or on WAT in mice fed a standard chow (Fig. 2*B*). On the other hand, LPS-induced activation of both JNK1 and JNK2 in peritoneal macrophages of the transgenic mice was markedly attenuated.

Likewise, HFD-induced elevation of JNK1 and JNK2 in the adipose tissue of the transgenic mice was also reduced to a level similar to that in lean mice, suggesting that transgenic expression of *dn-JNK* driven by the aP2 promoter is sufficient to inhibit the activation of both endogenous JNK1 and JNK2 in adipocytes and macrophages.

Adipose tissue–selective inactivation of JNK protects against HFD-induced obesity and its related metabolic disorders. On the standard chow, there was no obvious difference in body weight gain between the *ap2-dn-JNK* mice and their wild-type littermates (Fig. 3*A*). The *ap2-dn-JNK* mice had much less HFD-induced weight gain compared with age-matched littermates, with the difference in body weight being significant from the age of 10 weeks, despite similar caloric intake (Fig. 3*B*). The various fat depots weighed less in the *ap2-dn-JNK* mice, being significantly different from those of wild-type littermates in both WAT (subcutaneous and perirenal depots) and interscapular BAT (Fig. 3*C*). The adiposity index of *ap2-dn-JNK* mice was significantly reduced, compared with their wild-type littermates ($P < 0.05$) (Fig. 3*C*, *insert*), suggesting that *ap2-dn-JNK* mice were resistant to HFD-induced obesity.

Real-time PCR analysis demonstrated that the expression of several genes involved in adipogenesis, including necdin, preadipocyte factor, peroxisome proliferator–activated receptor-γ, CCAAT/enhancer-binding protein-α, and A-FABP, was not significantly different between *ap2-dn-JNK* mice and their wild-type littermates on an HFD in several types of adipose tissue (Supplementary Fig. 1), suggesting that JNK inactivation in adipose tissue did not impair adipocyte differentiation. On the other hand, histological analysis revealed that the *ap2-dn-JNK* mice had smaller adipocytes in the epididymal fat pads, as well as in BAT (Fig. 3*D* and *E*). Furthermore, the triglyceride contents of WAT and BAT were significantly reduced in *ap2-dn-JNK* mice, relative to their wild-type littermates (Fig. 3*F*).

The *ap2-dn-JNK* mice are protected from HFD-induced insulin resistance and glucose intolerance. An intraperitoneal glucose test was performed to compare the glucose tolerance of *ap2-dn-JNK* and wild-type mice. When fed with a standard chow, there was no obvious difference between the two groups of mice (Fig. 4*A*). In contrast, the *ap2-dn-JNK* transgenic mice were protected from HFD-induced glucose intolerance (Fig. 4*B* and *C*). The intraperitoneal insulin tolerance test also showed no significant difference in insulin sensitivity in the two groups of mice on the standard chow (Fig. 4*D*) but significantly better insulin sensitivity in the *ap2-dn-JNK* mice on HFD (Fig. 4*E* and *F*). The beneficial metabolic effects observed in the *ap2-dn-JNK* transgenic mice also included lower fasting glucose and insulin levels and homeostasis

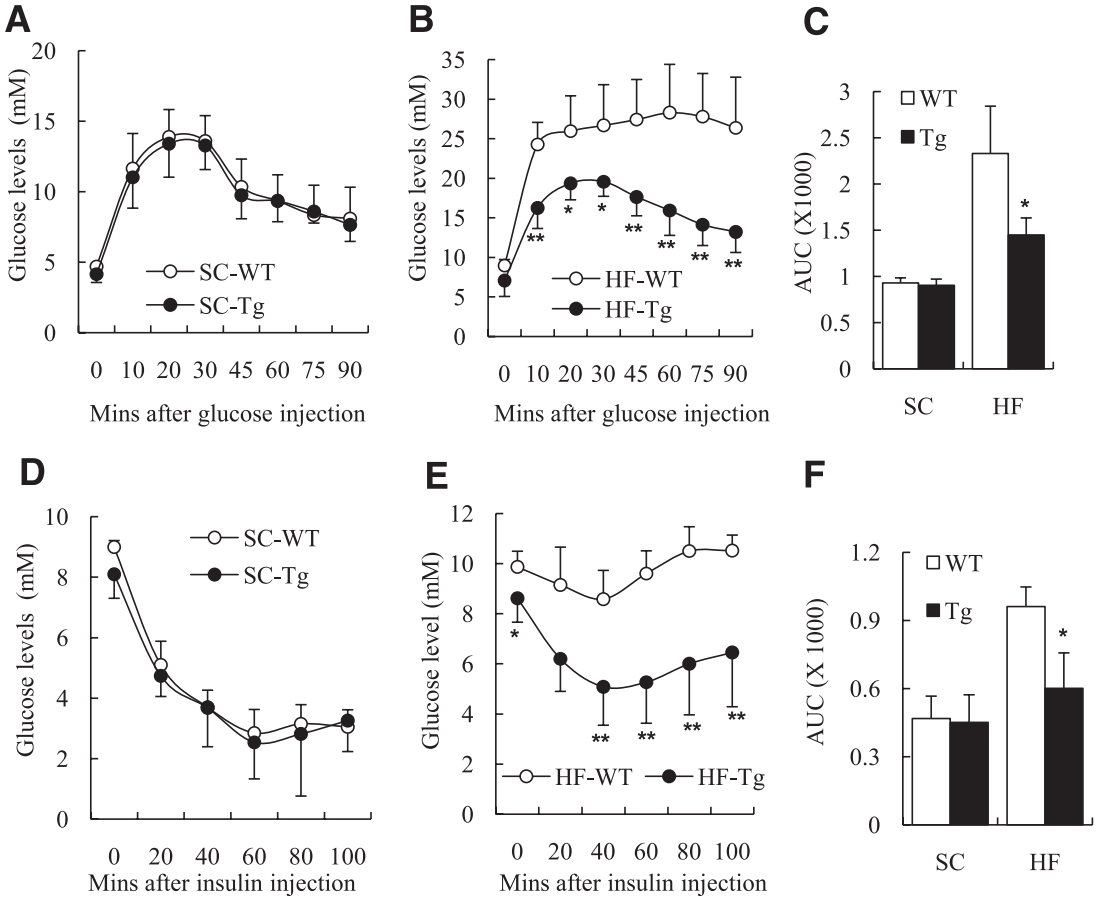

FIG. 4. Adipose tissue–selective inactivation of JNK improves in vivo glucose homeostasis and insulin sensitivity. The in vivo glucose homeostasis and insulin sensitivity were examined in *aP2-dn-JNK* transgenic (Tg) mice and their wild-type (WT) littermates at the age of 24 weeks while on standard chow (SC) or the HFD (HF) diet for 20 weeks. *A–C*: Glucose tolerance test (GTT). Mice fasted overnight were injected intraperitoneally with glucose (1 mg/g). Blood glucose concentration was measured at the indicated times in standard chow group (*A*), HFD-fed group (*B*), and represented as the area under the curve (*C*). *D–F*: Insulin tolerance test (ITT). Mice fasted overnight were injected intraperitoneally with insulin (0.75 mU/g). Blood glucose concentration was measured at the indicated times in standard chow (*D*) and HFD-fed (*E*) mice and represented as the area under the curve (*F*).

model assessment of insulin resistance index on the HFD (Supplementary Table 2).

Inactivation of JNK increases insulin-stimulated glucose uptake in skeletal muscles. We next investigated whether the improvement in insulin-mediated glucose uptake in skeletal muscle contributed to the phenotypic changes in the transgenic mice. This analysis showed that there were no significant differences in the basal rates of Akt phosphorylation (Thr308) and glucose uptake between the *aP2-dn-JNK* and wild-type mice in either soleus (Fig. 5*A* and *B*) or extensor digitorum longus muscles (data not shown) when fed either a standard chow or HFD. In wild-type *ob/ob* mice on an HFD, insulin-evoked Akt phosphorylation and glucose uptake were decreased by approximately 55 and 61%, respectively, compared with lean controls (Fig. 5*A* and *B*). In contrast, the levels of insulin-stimulated Akt phosphorylation and glucose uptake in the transgenic mice on the HFD were comparable to those in lean mice fed a standard chow, suggesting that the protection against HFD-induced glucose tolerance in the transgenic mice was attributed, at least in part, to an increase in insulin-evoked glucose uptake in skeletal muscle. Likewise, HFD-induced phosphorylation of JNK1/2 in skeletal muscle of the transgenic mice was significantly attenuated compared with wild-type littermates (Fig. 5*C*). HFD-induced impairment in insulin-stimulated glucose uptake in epididylmal WAT was also reversed in the transgenic mice (Supplementary Fig. 2).

Inactivation of JNK attenuates HFD-induced hepatic steatosis and glucose production. In the *aP2-dn-JNK* transgenic mice on HFD, the livers were smaller and reddish in color, in contrast to the livers from their wild-type littermates, which were bigger and had a yellowish-white color. The ratio of the liver to body weight was significant lower in the transgenic mice (Fig. 6*A*). To further investigate the effects of overexpression of *dn-JNK* on HFD-induced hepatic steatosis, we performed a hematoxylin and eosin and oil red o staining analysis. As shown in Fig. 6*B*, HFD induced a marked accumulation of lipid droplets in hepatic cells accompanied by a loss of normal cell morphology. Liver sections from *aP2-dn-JNK* transgenic mice, in contrast, displayed a normal morphology and an obvious reduction in the number of lipid-engorged hepatic cells, similar to those in lean controls (Fig. 6*B*).

Compared with the wild-type mice, the *ap2-dn-JNK* transgenic mice on the HFD had a significantly lower glucose production in response to pyruvate challenge (Fig. 6*C*). The mRNA levels of the two key hepatic gluconeogenic genes, including *PEPCK* and *G6Pase*, were significantly decreased in *aP2-dn-JNK* mice (Fig. 6*D*). Furthermore, transgenic expression of dn-JNK in adipose tissue also reversed HFD-induced impairment in phosphorylation of Akt (Thr308) and elevation in phosphorylation of JNK1/2 (Supplementary Fig. 3*A* and *B*).

Suppression of JNK reduces systemic and adipose tissue–specific inflammation. To investigate the role of JNK in HFD-induced macrophage infiltration and aberrant production of adipokines in the adipose tissue, we examined the expression of inflammatory markers in adipose tissue and adipokines in blood from HFD-fed *aP2-dn-JNK* and wild-type mice. The mRNA expression of F4/80, a macrophage marker, and several proinflammatory cytokines including IL-6, TNF-α, and MCP-1, were decreased in the transgenic mice, compared with the wild-type mice (Fig. 7*A*). This was further confirmed by immunohistochemisty using an anti-F4/80 antibody, showing that *aP2-dn-JNK* mice had a markedly decreased macrophage infiltration in adipose tissue (Fig. 7*B*). Furthermore, the transgenic mice with *dn-JNK* expression in adipose tissue on HFD feeding had significantly lower serum levels of leptin and A-FABP but higher levels of adiponectin, compared with their wild-type littermates (Fig. 7*C*).

Adipose tissue inactivation of JNK increases energy expenditure and lipid oxidation. To explore whether increased energy expenditure contributed to the reduced adiposity in *aP2-dn-JNK* mice, indirect calorimetry measurements were performed in mice that had been on the HFD for 2 weeks before the onset of obesity. The rate of oxygen consumption (V_{O_2}) was higher in *aP2-dn-JNK* mice over a 24-h period throughout the entire light/dark

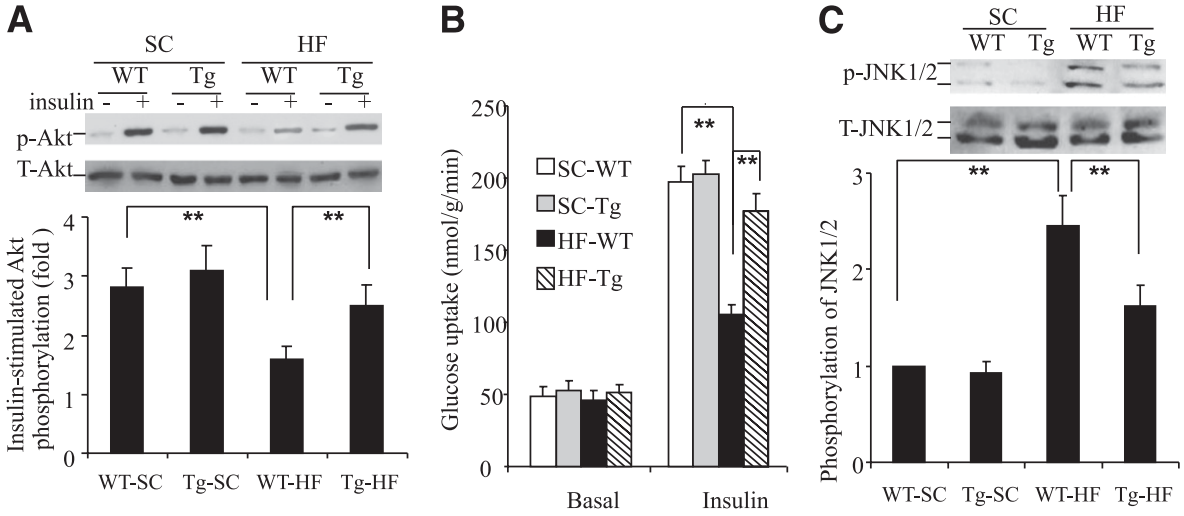

FIG. 5. Effect of adipose tissue–selective JNK activation on HFD-induced impairment in insulin signaling in skeletal muscle. *A*: The soleus muscle isolated from *aP2-dn-JNK* transgenic (Tg) mice and wild-type (WT) littermates at 16 weeks after the HFD (HF) or standard chow (SC) were treated with insulin (60 μU/mL) for 10 min, followed by Western blot analysis for phosphorylated Akt (Thr308) and total Akt. *B*: Glucose uptake in soleus muscle expressed as nmol/g wet weight/min. *C*: Western blot analysis for total and phosphorylated JNK1/2 in soleus muscle. The bar chart below represents the quantitative analysis for fold changes in JNK1/2 phopshorylation relative to lean controls. *$P < 0.05$; **$P < 0.01$; ***$P < 0.001$ ($n = 5$–6).

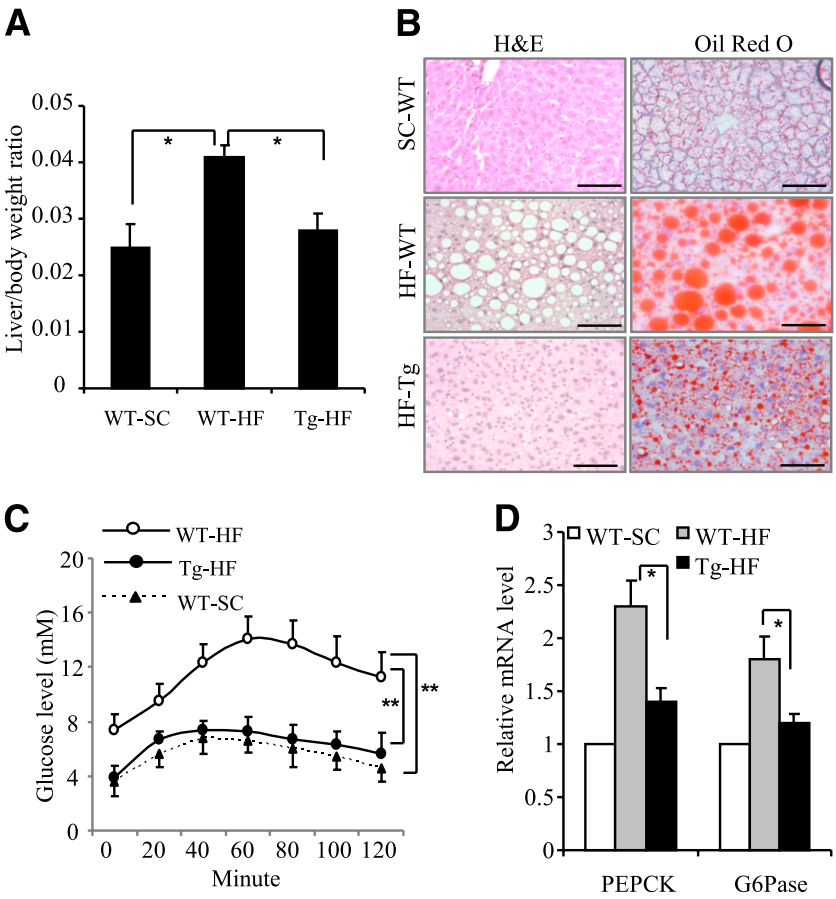

FIG. 6. Effect of adipose tissue–specific JNK inactivation on HFD-induced changes in the liver. *aP2-dn-JNK* transgenic (Tg) mice and their wild-type (WT) littermates were studied at the age of 24 weeks after 20 weeks of being fed with an HFD (HF) or standard chow (SC). *A*: The ratio of the liver to total body weight (n = 9–13). *B*: Representative histological sections of liver stained with hematoxylin and eosin and Oil Red O. Scale bar: 50 μm. *C*: *aP2-dn-JNK* transgenic mice and wild-type littermates fasted overnight were injected intraperitoneally with pyruvate (1 mg/g). Blood glucose concentration was measured at the indicated times (n = 6). *D*: Total RNA was isolated from the liver and the mRNA expression levels of *PEPCK* and *G6Pase* genes were examined by quantitative RT PCR. The data were normalized against the amount of 18S rRNA in each sample. *P < 0.05; **P < 0.01 (n = 9–13). (A high-quality digital representation of this figure is available in the online issue.)

cycle, reflecting an increase in energy expenditure during the whole day (Fig. 8*A*). The respiration exchange rate (V_{CO_2}/V_{O_2}) was significantly reduced in *aP2-dn-JNK* mice, indicating an increase in lipid utilization (Fig. 8*B*). These data revealed a significant change at the level of energy expenditure, together with an overall higher rate of lipid oxidation and the preferential use of fat as a fuel source, both of which might contribute to the reduced adiposity in the transgenic mice.

DISCUSSION

The central role of JNK in the pathogenesis of obesity, insulin resistance, and type 2 diabetes was first suggested by the demonstration that deletion of the *JNK1* gene (*JNK1*$^{-/-}$) leads to decreased adiposity and significant improvements in insulin sensitivity in both dietary and genetic (*ob/ob*) mouse models of obesity (8). Subsequent studies using targeted gene deletion (12,14) or reciprocal adoptive transfer (13) approaches had provided evidence for the contribution of *JNK1* inactivation in the adipocytes (14), skeletal muscles (12), and myeloid cells, such as macrophages (14), to the protection against HFD-induced insulin resistance seen in the *JNK1*$^{-/-}$ mice. However, none of these subsequent studies with these approaches for selective *JNK1* deletion could reproduce the protection from obesity evident in the conventional *JNK1*$^{-/-}$ mice. Similarly, the adenovirus-mediated hepatic overexpression of a dominant-negative (dn) form of JNK (11) also led to the improvement in whole-body insulin resistance, largely secondary to a reduction in hepatic glucose production. Again, this model of JNK inactivation in the liver, albeit only for 2 weeks, had no effect on weight gain in the treated animals. The identity of the cell type responsible for the resistance to obesity in the *JNK*$^{-/-}$ mice remains unknown. In this study, we have demonstrated that in the *ap2-dn-JNK* transgenic mice, selective inactivation of both JNK1 and JNK2 in the adipose tissue and macrophages can reproduce all the beneficial metabolic effects observed in the *JNK1*$^{-/-}$ mice, including protection from HFD-induced adiposity.

It should be noted that the resistance to obesity, together with enhanced insulin signaling, was also demonstrated in the mice with heterozygous *JNK1* deletion together with complete *JNK2* deletion (*JNK*$^{+/-}$ *JNK2*$^{-/-}$) (10). The authors concluded that the most critical determinant of insulin sensitivity, inflammation, and overall weight gain in the mice on HFD is likely to be total JNK kinase activity. The findings of our study suggest that the selective suppression of total JNK kinase activity, including inactivation of both JNK1 and JNK2, in adipose tissue, resulting from the combined downregulation of JNK in adipocytes and macrophages, is sufficient to

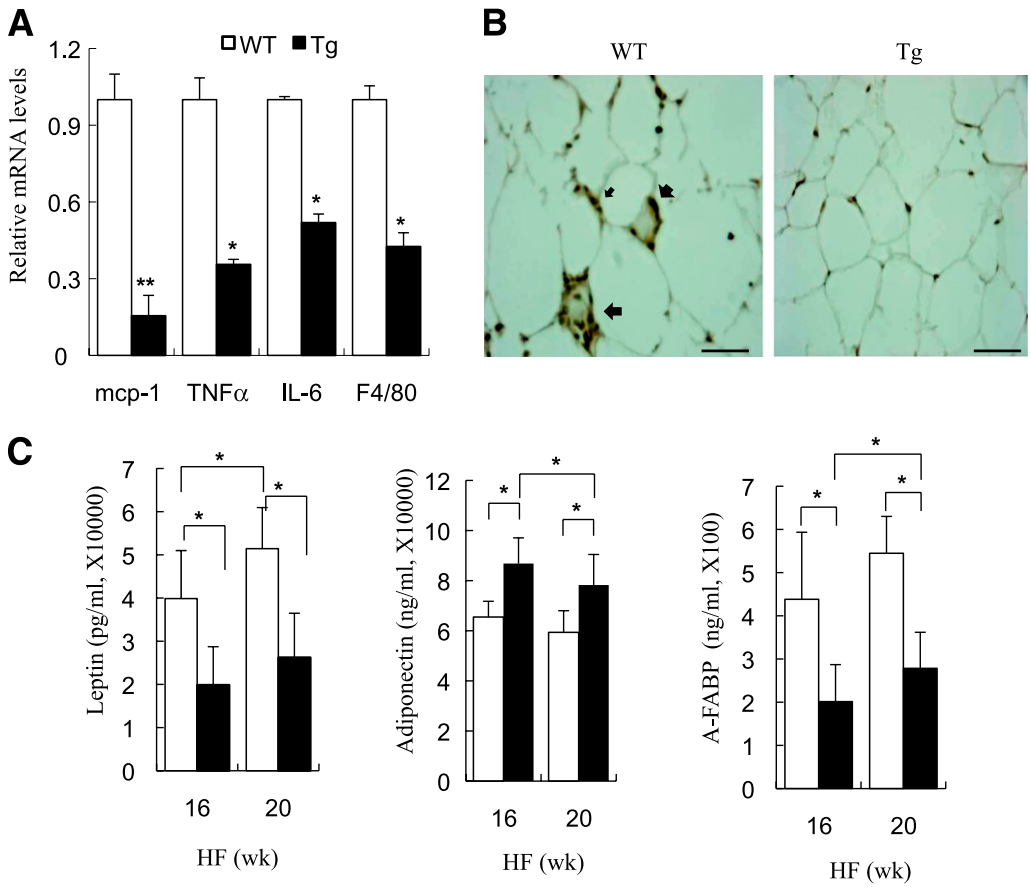

FIG. 7. Adipose tissue–specific inactivation of JNK alleviated the HFD-induced inflammatory changes. *A*: Quantitative RT PCR analysis for the gene expression of F4/80 and the inflammatory cytokines MCP-1, TNF-α, and IL-6 in epididymal fat. Expression levels of all genes were normalized against 18S rRNA. *B*: Immunohistochemical staining for F4/80 in epididymal fat tissue sections from *aP2-dn-JNK* transgenic (Tg) mice and wild-type (WT) littermates. Scale bar: 50 μm. *C*: Serum leptin, adiponectin, and A-FABP levels in overnight-fasted *aP2-dn-JNK* transgenic mice and wild-type littermates were measured by an enzyme-linked immunosorbent assay after being fed an HFD for 16 and 20 weeks, respectively. □, wild-type littermates; ■, *aP2-dn-JNK* transgenic mice. *$P < 0.05$; **$P < 0.01$ vs. wild-type littermates ($n = 6–8$). (A high-quality color representation of this figure is available in the online issue.)

reproduce the beneficial effects observed in the *JNK1*$^{-/-}$ or *JNK*$^{+/-}$ *JNK2*$^{-/-}$ mice. Previous studies have demonstrated considerable overlap in the biology and functions of the macrophages and adipocytes in obesity, which appear to be important for the high level of coordination between the inflammatory and metabolic pathways (2). Our study would support the importance of a cross-talk between the macrophages and adipocytes in mediating the effect of the JNK activation in diet-induced obesity. This information is of potential importance in drug development programs using JNK as a therapeutic target for obesity and type 2 diabetes.

In this study, the *ap2-dn-JNK* transgenic mice had decreased adipocyte size, which was also seen in the *JNK1*$^{-/-}$ mice (8). These transgenic mice had similar caloric intake as their wild-type littermates but had an increased rate of oxygen consumption and energy expenditure, findings that were also proposed to explain for the resistance to obesity in the *JNK1*$^{-/-}$ mice (13). A reduction in the respiration exchange rate in the *ap2-dn-JNK* transgenic mice, suggesting a preferential use of fat as a fuel source, provided another possible mechanism for their reduction in adiposity and triglyceride content in adipocytes. On the other hand, an impairment in adipocyte differentiation did not appear to play a significant role in the reduced fat mass in these transgenic animals.

The mechanism whereby inactivation of JNK in adipose tissue leads to increased energy expenditure remains unknown at this stage. In rodents, BAT is the primary site for energy dissipation (23). In diet-induced obesity, inflammation also occurs in BAT (24), which might impair its thermogenic functions by inducing mitochondria dysfunction. In our transgenic mice, the dn JNK is also expressed in high abundance in BAT. Therefore, it is possible that inactivation of JNK in BAT can restore the thermogenic activities impaired by the HFD. This hypothesis is currently under investigation in our laboratory.

On the HFD, the *ap2-dn-JNK* transgenic mice in this study had improved glucose tolerance and insulin sensitivity compared with their wild-type littermates. Their improvement in insulin sensitivity was accompanied by enhanced insulin-stimulated glucose uptake in the skeletal muscles, as well as reduced glucose production in response by the liver to pyruvate challenge. They were also protected against HFD-induced hepatosteatosis and had reduced expression of the genes involved in gluconeogenesis, compared with HFD-fed wild-type littermates. In a previous study, mice with selective adipocyte deletion of the *JNK1* gene also exhibited a protection against hepatosteatosis and hepatic insulin resistance but had no improvement in skeletal muscle insulin action. Furthermore, in the adipocyte-specific *JNK1*$^{-/-}$ mice, the degree

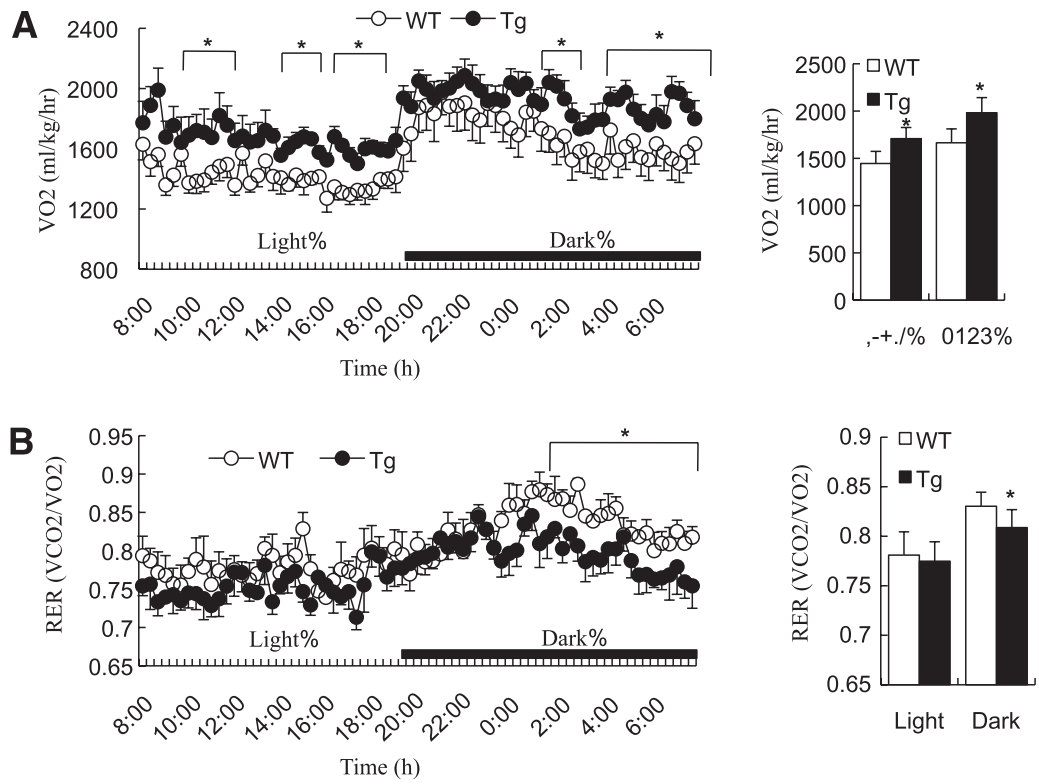

FIG. 8. Increased whole-body energy expenditure and lipid utilization in *aP2-dn-JNK* mice. Indirect calorimetry was performed using a six-chamber comprehensive laboratory animal monitoring system (Columbus Instruments). *A*: Whole-body oxygen consumption rate (V_{O_2}) was measured during the course of the daytime and night (*left*) and expressed as the average V_{O_2} over 24 h (*right*). *B*: Respiratory exchange rate (RER) was measured during the course of the daytime and night (*left*) and expressed as the average RER over 24 h (*right*). All 6-week-old mice were on an HFD for 2 weeks, starting from the age of 4 weeks. *$P < 0.05$; **$P < 0.01$ vs. wild-type littermate control mice (n = 6–8). Tg, *aP2-dn-JNK* transgenic mice; WT, wild-type littermates.

of macrophage infiltration in the adipose tissue was similar to wild-type mice and only the production of IL-6, but not TNF-α, was reduced relative to the wild-type mice. It is obvious that the *ap2-dn-JNK* transgenic mice in our study exhibited a much more marked protection against the inflammatory changes induced by the HFD. Not only was there a marked reduction in macrophage infiltration in the adipose tissue, there was also evidence of reduced expression of various proinflammatory cytokines and hormones, including TNF-α, MCP-1, A-FABP, and leptin in addition to IL-6. On the other hand, the circulating level of the anti-inflammatory adipokine, adiponectin, was increased. JNK activation on the HFD was also reduced in the liver and skeletal muscle, probably secondary to the reduced circulating levels of JNK-activating adipokines, such as TNF-α (9) and A-FABP (20), or to the decreased lipid contents in these tissues. These data suggest that the suppression of JNK activation in both the adipocytes and macrophages is required for the protection against HFD-induced insulin resistance in the skeletal muscles, probably consequent to the amelioration of adipose tissue inflammation and adipokine dysregulation.

In conclusion, this study has provided the first evidence that selective suppression of both JNK1 and JNK2 activation in adipose tissue and macrophages can protect against diet-induced obesity, through an increase in energy expenditure and fat utilization. Our data also support the importance of the cross-talk between the inflammatory and metabolic pathways mediated by macrophages and adipocytes in the development of obesity, insulin resistance, and type 2 diabetes.

ACKNOWLEDGMENTS

This work was supported by a general research fund grant from the Hong Kong Research Grant Council (767208M; to K.S.L.L.) and the Collaborative Research Fund (HKU 2/07C) and the National Basic Research Program of China (2011CB504004). No potential conflicts of interest relevant to this article were reported.

X.Z. researched data and wrote the manuscript. A.X. contributed to discussion and reviewed and edited the manuscript. S.K.C., G.S., and A.L. reviewed and edited the manuscript. J.H.B.C. and R.L.C.W. researched data. K.S.L.L. wrote, reviewed, and edited the manuscript.

REFERENCES

1. Bouloumié A, Curat CA, Sengenès C, Lolmède K, Miranville A, Busse R. Role of macrophage tissue infiltration in metabolic diseases. Curr Opin Clin Nutr Metab Care 2005;8:347–354
2. Wellen KE, Hotamisligil GS. Inflammation, stress, and diabetes. J Clin Invest 2005;115:1111–1119
3. Liu S, Tinker L, Song Y, et al. A prospective study of inflammatory cytokines and diabetes mellitus in a multiethnic cohort of postmenopausal women. Arch Intern Med 2007;167:1676–1685
4. Xu A, Wang Y, Keshaw H, Xu LY, Lam KS, Cooper GJ. The fat-derived hormone adiponectin alleviates alcoholic and nonalcoholic fatty liver diseases in mice. J Clin Invest 2003;112:91–100
5. Xu A, Wang Y, Xu JY, et al. Adipocyte fatty acid-binding protein is a plasma biomarker closely associated with obesity and metabolic syndrome. Clin Chem 2006;52:405–413
6. Bennett BL, Satoh Y, Lewis AJ. JNK: a new therapeutic target for diabetes. Curr Opin Pharmacol 2003;3:420–425
7. Davis RJ. Signal transduction by the JNK group of MAP kinases. Cell 2000; 103:239–252

8. Hirosumi J, Tuncman G, Chang L, et al. A central role for JNK in obesity and insulin resistance. Nature 2002;420:333–336
9. Ozcan U, Cao Q, Yilmaz E, et al. Endoplasmic reticulum stress links obesity, insulin action, and type 2 diabetes. Science 2004;306:457–461
10. Tuncman G, Hirosumi J, Solinas G, Chang L, Karin M, Hotamisligil GS. Functional in vivo interactions between JNK1 and JNK2 isoforms in obesity and insulin resistance. Proc Natl Acad Sci USA 2006;103:10741–10746
11. Nakatani Y, Kaneto H, Kawamori D, et al. Modulation of the JNK pathway in liver affects insulin resistance status. J Biol Chem 2004;279:45803–45809
12. Sabio G, Kennedy NJ, Cavanagh-Kyros J, et al. Role of muscle c-Jun NH2-terminal kinase 1 in obesity-induced insulin resistance. Mol Cell Biol 2010;30:106–115
13. Solinas G, Vilcu C, Neels JG, et al. JNK1 in hematopoietically derived cells contributes to diet-induced inflammation and insulin resistance without affecting obesity. Cell Metab 2007;6:386–397
14. Sabio G, Das M, Mora A, et al. A stress signaling pathway in adipose tissue regulates hepatic insulin resistance. Science 2008;322:1539–1543
15. Kaneto H, Nakatani Y, Miyatsuka T, et al. Possible novel therapy for diabetes with cell-permeable JNK-inhibitory peptide. Nat Med 2004;10:1128–1132
16. Zheng C, Xiang J, Hunter T, Lin A. The JNKK2-JNK1 fusion protein acts as a constitutively active c-Jun kinase that stimulates c-Jun transcription activity. J Biol Chem 1999;274:28966–28971
17. Zhang X, Lam KS, Ye H, et al. Adipose tissue-specific inhibition of hypoxia-inducible factor 1alpha induces obesity and glucose intolerance by impeding energy expenditure in mice. J Biol Chem 2010;285:32869–32877
18. Cheng KK, Iglesias MA, Lam KS, et al. APPL1 potentiates insulin-mediated inhibition of hepatic glucose production and alleviates diabetes via Akt activation in mice. Cell Metab 2009;9:417–427
19. Beck Jørgensen S, O'Neill HM, Hewitt K, Kemp BE, Steinberg GR. Reduced AMP-activated protein kinase activity in mouse skeletal muscle does not exacerbate the development of insulin resistance with obesity. Diabetologia 2009;52:2395–2404
20. Hui X, Li H, Zhou Z, et al. Adipocyte fatty acid-binding protein modulates inflammatory responses in macrophages through a positive feedback loop involving c-Jun NH2-terminal kinases and activator protein-1. J Biol Chem 2010;285:10273–10280
21. Xu H, Barnes GT, Yang Q, et al. Chronic inflammation in fat plays a crucial role in the development of obesity-related insulin resistance. J Clin Invest 2003;112:1821–1830
22. Maeda K, Uysal KT, Makowski L, et al. Role of the fatty acid binding protein mal1 in obesity and insulin resistance. Diabetes 2003;52:300–307
23. Lowell BB, Spiegelman BM. Towards a molecular understanding of adaptive thermogenesis. Nature 2000;404:652–660
24. Hageman RS, Wagener A, Hantschel C, Svenson KL, Churchill GA, Brockmann GA. High-fat diet leads to tissue-specific changes reflecting risk factors for diseases in DBA/2J mice. Physiol Genomics 2010;42:55–66